ELSEVIER

Surface Science 361/362 (1996) 138–141

surface science

Tuning a double quantum well Fermi surface with in-plane magnetic fields

J.A. Simmons *, N.E. Harff, T.M. Eiles, S.K. Lyo, J.F. Klem

Sandia National Laboratories, Albuquerque, NM 87185-1415b, USA

Received 31 May 1995; accepted for publication 22 September 1995

Abstract

A double quantum well (QW) subject to in-plane magnetic fields $B_{||}$ has the dispersion curves of its two QWs shifted in k-space. When the QWs are strongly coupled, an anticrossing and partial energy gap occur, yielding a tunable multi-component Fermi surface. We report measurements of the resultant features in the conductance, the capacitive density of states and giant deviations in the cyclotron effective masses.

Keywords: Conductivity; Electrical transport measurements; Gallium arsenide; Magnetic phenomena; Quantum wells; Tunneling

Double quantum wells (DQWs) constitute a system in which an additional degree of freedom can be controllably introduced to a two-dimensional electron gas by changing the thickness and height of the grown interwell barrier. For purely in-plane fields $B_{||}$, single particle tunneling dynamics dominate the interactions, with the primary effect of $B_{||}$ being a linear transverse shift in the momenta $\hbar k$ of electrons in one QW relative to those in the other [1,2].

Here we describe our studies of a strongly coupled DQW subject to a high $B_{||}$. The strong tunneling causes the shifted QW dispersion curves to distort into an anticrossing, opening a partial energy gap or minigap. This mixes the two (displaced) QW Fermi circles to produce a Fermi Surface (FS) with two orbits of greatly differing area. At the edges of the gap, van Hove singularities in the density of states $D(\epsilon)$ appear, and electron group velocities approach zero. By sweeping $B_{||}$, the FS can be tuned and the gap made to pass through the chemical potential μ, with the gap edges producing dramatic effects in the transport properties [3,4]. These include sharp features in the conductance and capacitance, and giant deviations in the cyclotron mass m_c.

The two samples studied were grown by MBE. Each sample, A (B), consisted of a modulation-doped pair of GaAs QWs of equal width [$w=$ 150 Å (100 Å)] separated by an $Al_{0.3}Ga_{0.7}As$ barrier of thickness $t=25$ Å (35 Å). Each QW had density $n\approx 1.5\times 10^{11}$ (1.2×10^{11}) cm^{-2} as measured by Shubnikov-de Haas oscillations (SdHO) for $B_{||}=0$. Top and bottom QW mobilities were ≈ 2.7 and ≈ 2.2 x 10^5 (≈ 1.2 and $\approx 0.6\times 10^5$) cm^2 V^{-1} s^{-1}. Four-terminal 17 Hz lock-in resistance measurements were performed on Hall bars with

* Corresponding author. Fax: +1 505 8441197; e-mail: jsimmon@sandia.gov.

0039-6028/96/$15.00 Copyright © 1996 Elsevier Science B.V. All rights reserved
PII S0039-6028(96)00353-6

Cr/Au top gates and the excitation current parallel to $B_\parallel$. Measurements of m_c required a simultaneous small $B_\perp$ and large $B_\parallel$, achieved by applying a uniform total field B_T at angles $\theta = 0°$, 2.5°, 3.0° and 3.5° from parallel, with rotations performed in situ.

Fig. 1a shows the normalized in-plane resistance $R_\parallel(B_\parallel)$ for sample A, at zero gate bias, $T = 0.5$ K and $\theta = 0$. A minimum occurs at 5.9 T, followed by a maximum at 6.5 T. We now discuss the origin of these two features [3,4]. Fig. 2a shows a tight-binding calculation for sample A of the DQW dispersion $\epsilon(k_y)$, for $B_\parallel = 7.5$ T in the x-direction [5]. $B_\parallel$ shifts the QW dispersion curves relative to

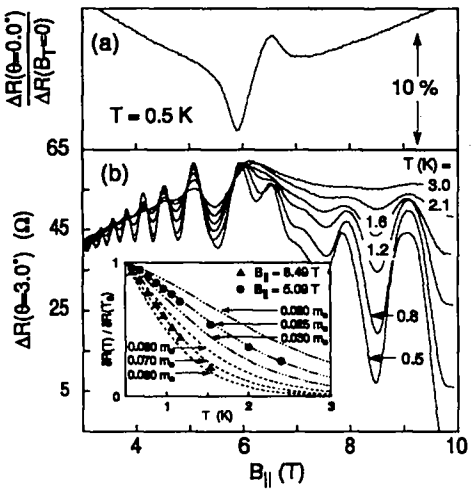


Fig. 1. (a) Normalized $R_\parallel(B_\parallel)$ of sample A at $\theta = 0$ and zero gate bias. (b) $\Delta R(B_\parallel, \theta = 3.0°)$ for several T. Inset: SdHO amplitudes versus T, and fits to Eq. (1), for two $B_\parallel$.

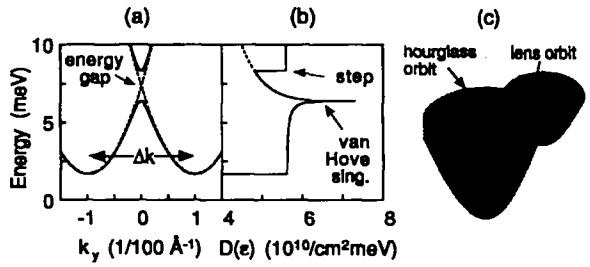


Fig. 2. Sample A calculations at $B_\parallel = 7.5$ T. (a) $\epsilon(k_y)$ with (solid lines) and without (dotted lines) coupling. (b) $D(\epsilon)$ for the lower energy branch (dotted line) and both branches (solid line). (c) Sketch of the dispersion curve and Fermi surface at 7.5 T for $\mu \approx 9$ meV.

one another by an amount $\Delta k_y = edB_\parallel/\hbar$. The strong coupling produces an anticrossing and minigap whose width ϵ_G (of order 1 meV) is independent of $B_\parallel$ and $\approx \Delta_{SAS}$, the zero-field symmetric-antisymmetric gap [6]. The minigap dramatically distorts $D(\epsilon)$ and the electron group velocities (Fig. 2b). Since the upper branch of $\epsilon(k)$ is nearly parabolic, a step-like increase occurs in D(ϵ) at the upper gap edge. Thus as $B_\parallel$ is increased, the (low velocity) states at the upper gap edge pass through μ and are abruptly emptied, reducing scattering and causing a sharp minimum in $R_\parallel$. By contrast, $\epsilon(k)$ at the lower gap edge is saddle-shaped, yielding a logarithmic divergence in $D(\epsilon)$. When the lower gap edge crosses μ at higher $B_\parallel$, electrons are divergently scattered into these (zero-velocity) states, yielding the maximum in $R_\parallel$.

The shape of the FS is given by the intersection of μ and $\epsilon(k)$. For $B_\parallel < 5.9$ T, μ lies above the gap and the FS has a small lens-shaped orbit lying within a larger hourglass-shaped orbit, as shown in Fig. 2c. For $5.9\ \text{T} < B_\parallel < 6.5$ T, μ lies in the gap and only the hourglass orbit is present. As $B_\parallel$ is increased further, μ touches the lower gap edge, causing the hourglass "waist" to pinch off. For $B_\parallel > 6.5$ T, the FS separates into two Fermi circles of roughly equal size.

The changes $\Delta D(\epsilon)$ in $D(\epsilon)$ were measured directly via the changes $\Delta C(B_\parallel)$ in the capacitance between the surface gate and the DQW. For small values of $\Delta D(\epsilon)$ relative to the full 2D density of states, $\Delta C(B_\parallel) \propto \Delta D(\epsilon)$ [7]. This condition appears to hold for our sample, whose surface gate is located 1347 Å from the center of the interwell barrier. We used a low frequency (20–100 Hz) capacitance bridge technique at 300 mK, allowing an accuracy of ≈ 1 part in 10^4 at excitation voltages of 2–10 mV. In Fig. 3 we show $\Delta C(B_\parallel)$ of sample B (gate area ≈ 5.4 mm^2) for several different gate voltages. In contrast to the conductance data, $C(B_\parallel)$ remains relatively constant at low $B_\parallel$, until a sudden step-like decrease appears. This corresponds to the disappearance of the lens orbit, occurring when the upper gap edge crosses μ. The value of $C(B_\parallel)$ then increases monotonically, and ends in a slight peak before settling at a value nearly the same as at $B_\parallel = 0$. The peak is due to the lower gap edge, with a logarithmic singularity

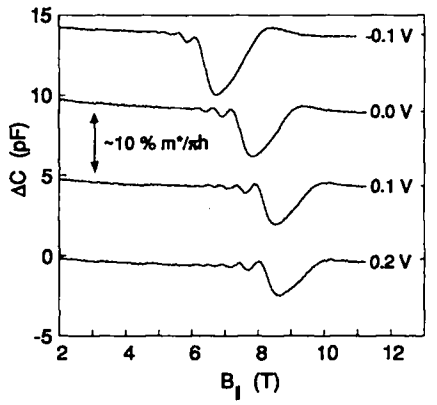


Fig. 3. The change in capacitance $\Delta C(B_\parallel)$, proportional to $\Delta D(\epsilon)$, of sample B for several gate biases, offset from one another by 5 pF. The curves are strikingly similar to Fig. 2b.

in $D(\epsilon)$, crossing μ, and is washed out due to damping. The relative constancy of $C(B_\parallel)$ outside the anticrossing region is in stark contrast to $R_\parallel$ (see Fig. 1a), which convolves the changing Fermi velocities. The shape of $C(B_\parallel)$ bears a striking resemblance to the calculated $D(\epsilon)$ of Fig. 2b. Thus a simultaneous measurement of capacitance and conductance may provide a method for the future study of the singular scattering dynamics of electrons in this system. The slight oscillations just below the step-decrease are SdHO due to an unintended slight misalignment of the sample from $\theta = 0°$.

By adding a small $B_\perp$ and measuring the temperature (T) dependence of the resulting SdHO, we probed m_c near the minigap [8]. $B_\parallel$ and $B_\perp$ could not be swept independently, mixing the SdHO with the anticrossing features. To remove this mixing, for each T examined we subtracted the resistance at $\theta = 0°$ (e.g., Fig. 1a from the resistance in a tilted field, to yield $\Delta R(B_\parallel,\theta) = R(B_\parallel,\theta) - R(B_\parallel,\theta = 0°)$. Fig. 1b shows $\Delta R(B_\parallel,\theta = 3.0°)$ for several T. The SdHO are uniform up to ≈ 5.9 T; then both the period and amplitude change significantly, indicating a drastic change in m_c. To determine m_c, we first consider which FS orbits contribute. For $B_\parallel < 5.9$ T, the lens and hourglass orbits enclose greatly different areas in k-space. Electrons traverse these orbits at a rate $d\boldsymbol{k}/dt = -(e/h)\boldsymbol{v}_k \times \boldsymbol{B}_\perp$, where $\boldsymbol{v}_k$ is the Fermi velocity. When $B_\perp$ is sufficiently small, electrons in the hourglass are unable to complete the orbit without scattering, contributing negligibly to the SdHO. However, because $\boldsymbol{v}_k$ is nearly the same for the two orbits (except very close to the gap edge), enough electrons complete the lens orbit to produce SdHO. This assumption agrees with the data for $B_\parallel < 5.9$ T, where only a single period occurs for all three θ. For $5.9\ \text{T} < B_\parallel < 6.5$ T, the FS consists of only the hourglass, while for $B_\parallel > 6.5$ T the FS consists of two separated Fermi circles of equal size, producing SdHO of the same period and T-dependence. Thus for all three ranges, the SdHO arises from a single orbit of the FS.

For a single FS orbit, when $B_\perp$ is sufficiently small, the SdHO are expected to become small in amplitude and sinusoidal in shape, with higher order terms becoming negligible. [9] This is in accord with our data, where the SdHO never exceed 15% of the background. In this case, the SdHO amplitude is given by

$$\frac{\delta R(T)}{\delta R(T_0)} = \frac{T \sin h(\beta T_0 (m_c/m_0)/B_\perp)}{T_0 \sin h(\beta T (m_c/m_0)/B_\perp)} \qquad (1)$$

where T_0 is base T, $\beta = 2\pi^2 k_B m_0/he$, and m_0 is the free electron mass. The Fig. 1b inset shows two typical fits of Eq. (1) to the $\theta = 3.0°$ data. (Here δR is obtained by taking the difference between $\Delta R(B_\parallel,\theta)$ evaluated at adjacent SdHO extrema, and subtracting the magnetoresistance background). While for 8.49 T the value of $m_c = 0.070\ m_0$, for 5.09 T it is $m_c = 0.025\ m_0$, a factor of three lower than m^*_{GaAs}. While in general the fits yield m_c to $\pm 10\%$ error, for the range $\approx 5.9 \leq B_\parallel \leq \approx 6.5$ T m_c is changing rapidly, and has roughly $\pm 20\%$ error.

Fig. 4 shows m_c versus ($B_\parallel$) for all three θ. At 2.7 T, $m_c \approx 0.050 m_0$, considerably lower than m^*_{GaAs}. Raising $B_\parallel$ causes m_c to decrease, reaching $0.021 m_0$ near the upper gap edge at 5.6 T. As $B_\parallel$ is increased further, m_c suddenly increases, reaching a value of $0.099 m_0$ just below 6.5 T, where μ crosses the lower gap edge, or saddle point; m_c then rapidly converges to m^*_{GaAs} near ≈ 7 T and remains roughly constant thereafter.

Following Lyo [10], an understanding of the behavior of m_c can be gained by examining Fig. 2 and employing the expression

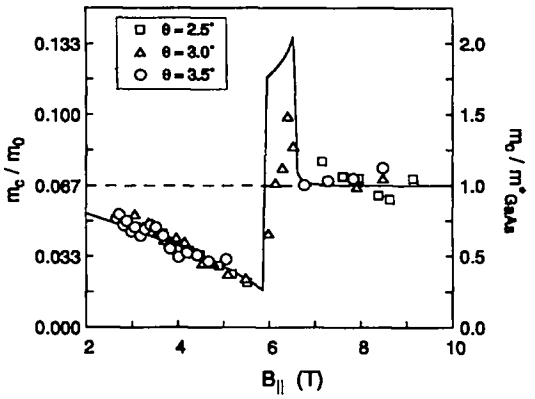


Fig. 4. Summary of measured m_c values versus $B_{||}$, for sample A. The solid line is the theoretical calculation of Ref. [10].

$m_c = (h/2\pi) \oint v^{-1}_k dk$, where the integration is along the dominant orbit. As $B_{||}$ is increased, the upper gap edge moves upward towards μ. As a result, the size of the lens orbit decreases, while v_k decreases more slowly, resulting in a monotonic decrease of m_c. The lens orbit vanishes at 5.9 T but, because v_k also vanishes, m_c does not go to zero. Above 5.9 T, the orbit size increases abruptly as electrons move to the hourglass orbit, causing an abrupt increase in m_c. As $B_{||}$ increases from 5.9 to 6.5 T, μ lies in the minigap and moves towards the saddle point. At the same time, v_k becomes smaller near the saddle-point, yielding now a monotonic increase of $m_c(B_{||})$. The divergence of m_c at the saddlepoint, due to v_k vanishing, is suppressed in the data by damping. Above 6.5 T μ falls below the saddle point, splitting the hourglass into two roughly circular orbits with nearly parabolic dispersion, and causing m_c to approach m^*_{GaAs}. In Fig. 4 we plot Lyo's calculation of $m_c(B_{||})$ for sample A, where $B_{||}$ has been scaled by 0.96. Excellent agreement is seen.

In summary, an anticrossing and minigap appear in strongly coupled DQWs subject to a strong $B_{||}$, giving rise to singularities in the density of states, sharp features in the resistance and gate capacitance and giant deviations in the cyclotron effective masses.

Acknowledgement

This work was supported by the US Department of Energy under Contract No. DE-AC04-94AL85000.

References

[1] J.P. Eisenstein, T.J. Gramila, L.N. Pfeiffer and K.W. West, Phys. Rev. B 44 (1991) 6511.
[2] J.A. Simmons, S.K. Lyo, J.F. Klem, M.E. Sherwin and J.R. Wendt, Phys. Rev. B 47 (1993) 15741; S.K. Lyo and J.A. Simmons, J. Phys. Condens. Mater. 5 (1993) L299.
[3] J.A. Simmons, S.K. Lyo, N.E. Harff and J.F. Klem, Phys. Rev. Lett. 73 (1994) 2256.
[4] S.K. Lyo, Phys. Rev. B 50 (1994) 4965.
[5] Including the Hartree term increases the center-to-center distance between the two QW wavefunctions, lowering the $B_{||}$ at which the minigap crosses μ and reducing ϵ_G.
[6] G.S. Boebinger, H.W. Jiang, L.N. Pfeiffer and K.W. West, Phys. Rev. Lett. 64 (1990) 1793.
[7] M. Buttiker, J. Phys. Condens. Mater. 5 (1993) 9361, and references therein.
[8] N.E. Harff, J.A. Simmons, S.K. Lyo, J.E. Schirber, J.F. Klem and S.M. Goodnick, in: The Physics of Semiconductors, Vol. 1, Ed. D.J. Lockwood (World Scientific, Singapore, 1995) p. 831.
[9] T. Ando, A.B. Fowler and F. Stern, Rev. Mod. Phys. 54 (1982) 437.
[10] S.K. Lyo, Phys. Rev. B 51 (1995) 11160.